Superlattices and Microstructures, Vol. 23, 1353 (1998)

Multistable current-voltage characteristics as fingerprints of growth-related imperfections in semiconductor superlattices

G. Schwarz, M. Patra, F. Prengel, and E. Schöll
Institut für Theoretische Physik, Technische Universität, Hardenbergstraße 36, D-10623 Berlin

(Received 15 July 1996)

The influence of imperfections and growth-related disorder on the current-voltage characteristics of doped superlattices is investigated theoretically. It is demonstrated that the location of a defect can be directly identified from the current measurements. Such measurements can also be used as an estimate for the degree of microscopic disorder.

1. Introduction

When sufficiently doped or optically excited, semiconductor superlattices exhibit the formation of electric field domains for charge transport along the growth direction. This gives rise to the occurrence of a multistable series of branches in the current-voltage characteristic, as has been demonstrated both experimentally [1, 2] and theoretically [3, 4]. While theoretical models which assume a "perfect" superlattice are able to explain the principal features observed in the experiments they yield a strictly regular sequence as opposed to the measured characteristics, where the different branches vary considerably in length.

Although seemingly random, those characterstics can be reproduced in detail, even for measurements on different superlattice samples of the same wafer [5]. It is thus reasonable to assume that the distinct irregular shape of a characteristic is the result of microscopic spatial fluctuations of growth parameters such as layer thickness or doping density along the growth direction. The observation that in-plane fluctuations like interface roughness obviously do not play a role for the individual shape of the current-voltage characteristic of a sample can be understood if one keeps in mind that their length scales of typically some nm [6] are small compared to the sample dimensions of the order of 100 μm (cf. e. g. [2]), so they are effectively averaged out.

2. Simulating disorder

As we are considering vertical transport in n-doped superlattices we can limit our calculations to a one-dimensional description of the conduction band. To simulate charge transport we use a simple rate equation model for the electron concentrations in the different quantum wells derived in Ref. [3] for the case of an "ideal" superlattice. In order to deal with varying layer thickness we introduce a "local" lattice constant $d_i := (l_i + l_{i-1})/2 + b_i$, where l_i and b_i are the widths of the i^{th} well

0749–6036/96/000000 + 00 $18.00/0

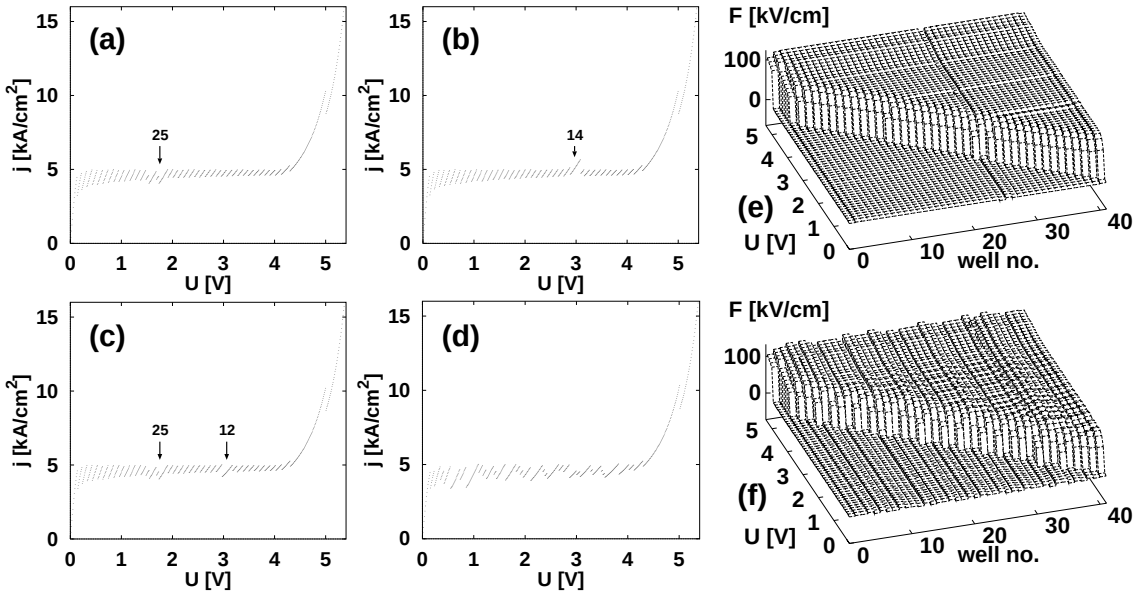

Fig. 1. Calculated current-voltage characteristics (a–d) of superlattice samples with different defects ($N = 40$ periods, doping density $N_D = 6.7 \cdot 10^{17}$ cm^{-3}). The numbers refer to the affected branches, counted from the right. In (a) the 25^{th} well is wider by one monolayer, in (b) the 14^{th} barrier is smaller. (c): smaller 12^{th} and wider 25^{th} well. (d): random distribution of 7 smaller and 7 wider wells. (e) and (f) show the spatial distribution of the electric field F as a function of the applied voltage U for (a) and (d), respectively (voltage sweep-up).

and barrier, respectively, which we employ in the expressions for electron transport across the i^{th} barrier. The inclusion of different doping densities $N_D^{(i)}$ for each well i into the original model via Poisson's equation is straightforward [5, 7].

For the widths of the individual layers of a sample we assume that they can deviate by one monolayer from the nominal values l and b of the well and barrier widths due to irregularities during the growth process. We thus use a sequence of N values $l_i \in \{l, l + \Delta l, l - \Delta l\}$ for the widths of the wells, as well as another sequence of $N - 1$ values $b_i \in \{b, b + \Delta b, b - \Delta b\}$ for the barriers. Here, N is the total number of superlattice periods, and Δl, Δb are the widths of one monolayer (≈ 2.8 Å for both GaAs and AlAs). The degree of disorder is then given by the number of smaller and wider wells (or barriers, respectively).

To simulate doping fluctuations we generate a random series of N values $e_i \in [-1, 1]$ and calculate the individual doping densities as $N_D^{(i)} = N_D(1 + \alpha e_i)$ with a nominal doping density N_D. The parameter α enables us to scale the degree of disorder without altering the individual sequence of wells with higher and lower doping.

3. Current-voltage characteristics of imperfect superlattices

We have calculated the $j(U)$ characteristics of a GaAs/AlAs superlattice with $N = 40$ periods, $l = 90$ Å, $b = 15$ Å and a nominal doping density of $N_D = 6.7 \cdot 10^{17}$ cm^{-3}. The principal results, however, do not depend on those specific values.

Fig. 1 (a) shows the current-voltage characteristic of a superlattice whose 25^{th} well is wider by one monolayer. One can clearly see that the periodic pattern of the sequence of branches is disrupted around branch no. 25, counted from the right. This can be explained with the help of the

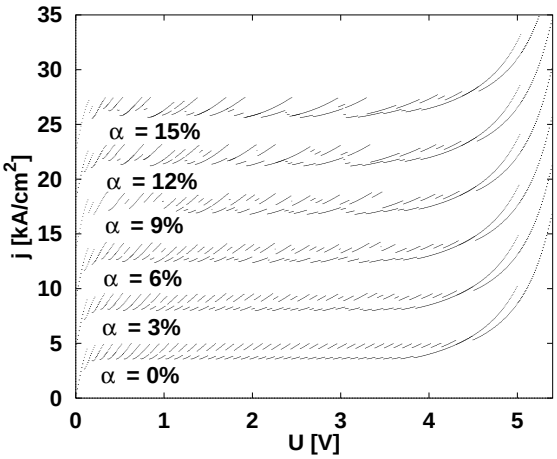

Fig. 2. Simulated characteristics of samples with different degree α of doping disorder (nominal doping density $N_D = 6.7 \cdot 10^{17}$ cm^{-3}). The upper curves are vertically shifted by 4.5 kA/cm^2 against one another. Both voltage sweep-up and sweep-down are shown.

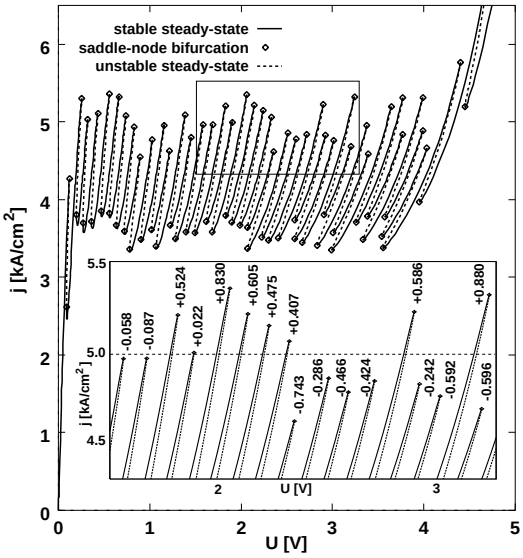

Fig. 3. Computed continuous characteristic of stable and unstable stationary states for the same doping density as in Fig. 2 with $\alpha = 8\%$. The inset shows an enlarged section (see text).

corresponding spatial field distribution depicted in Fig. 1 (e). While for very small voltages U an almost homogeneous field distribution exists, a high-field domain forms at the cathode (near well no. 40) for about $U = 0.1$ V. With increasing applied voltage this high field domain expands across the superlattice structure period by period. In the characteristic this leads to the occurrence of current branches, where consecutive branches correspond to a location of the electron accumulation (forming the domain boundary) in neighbouring quantum wells [2]. The field distribution shows that within both the high-field and low-field region the fields across the 25^{th} and 26^{th} barrier are slightly distorted. This is in order to compensate for the shift of the energy levels in the 25^{th} quantum well due to its different width, as the current across each barrier must be equal in the stationary state [5]. For the same reason the voltage at which the domain boundary expands across those periods is slightly changed compared to the case of a strictly periodic superlattice structure.

In Fig. 1 (b) the simulated characteristic of a sample with a thinner 14^{th} barrier is depicted. Again, we see a local deviation in the lengths of those two branches that correspond to the wells adjacent to the perturbation. To satisfy current conservation the field across the thinner barrier must be lower than elsewhere, which, like in (a), leads to a shift in the voltage at which the domain boundary crosses that period. In a sample with multiple defects each of them has a local effect in the characteristic, and they can still be localized easily (cf. Fig. 1 (c)). Only if the number of imperfections is so large that the periodicity of the sample is lost and the influences of adjacent perturbations on the field distribution interact, they can no longer be distinguished in the characteristic (Figs. 1 (d), (f)).

Fig. 2 shows the current-voltage characteristics of samples with doping fluctuations. While the sequence e_i is the same for all simulations, different degrees of disorder α have been used. Accordingly, the specific sequence of longer and shorter branches remains the same, whereas the variations in the lengths of the branches increase with α, and some of the smaller branches are not at all

visible in case of voltage sweep-up or sweep-down for higher degrees of disorder. It is thus possible to estimate α from the degree of fluctuation in the lengths of the branches.

4. Quantitative analysis

Instead of numerically solving the time-dependent rate equations with appropriate initial conditions one can also directly compute the fixed points of the dynamic system, i. e. its (stable or unstable) stationary states. Fig. 3 demonstrates that the different branches visible in the simulated (or measured) up-sweep and down-sweep characteristics are part of a single continuously connected stationary characteristic whose stability alternates via saddle-node bifurcations. It can be shown that the current density j at any such bifurcation which marks the end of a stable branch is directly related to the doping density of the respective well. To illustrate this, we have labeled each branch in the inset of Fig. 3 with the relative deviation e_i of the corresponding well from the nominal doping density of $N_D = 6.7 \cdot 10^{17}$ cm^{-3}. The dotted horizontal line corresponds to a perfect superlattice, i. e. $N_D^{(i)} = N_D$. The larger the deviation of the local doping density is, the more differs the current density j at the corresponding bifurcation point from that dotted line. Thus the degree of disorder can be directly read off from the maximum currents of the different branches.

5. Conclusions

In conclusion we have demonstrated that microscopic growth-related disorder and imperfections have a direct influence on the detailed shape of the macroscopic current-voltage characteristic. With increasing voltage the domain boundary scans the sample period by period from the cathode to the anode. The resulting current-voltage characteristic thus represents a "fingerprint" of the growth-related imperfections where the voltage at which a deviation from the periodic branch structure occurs is directly related to the spatial location of an imperfection within the sample.

For the case of doping fluctuations we have shown a direct relationship between the height of a current branch and the doping concentration in the corresponding well of the superlattice. If the type of microscopic disorder is known, current-voltage measurements can thus yield a quantitative estimate for the degree of those fluctuations.

The authors are indebted to A. Wacker, J. Kastrup, H. T. Grahn, and Y. Zhang for their collaboration. This work was supported in part by DFG in the framework of Sfb 296.

References

[1] H. T. Grahn, R. J. Haug, W. Müller, and K. Ploog, Phys. Rev. Lett. **67**, 1618 (1991).
[2] J. Kastrup, H. T. Grahn, K. Ploog, F. Prengel, A. Wacker, and E. Schöll, Appl. Phys. Lett. **65**, 1808 (1994).
[3] F. Prengel, A. Wacker, and E. Schöll, Phys. Rev. B **50**, 1705 (1994).
[4] L. L. Bonilla, J. Galán, J. A. Cuesta, F. C. Martínez, and J. M. Molera, Phys. Rev. B **50**, 8644 (1994).
[5] G. Schwarz, A. Wacker, F. Prengel, E. Schöll, J. Kastrup, H. T. Grahn, and K. Ploog, Semicond. Sci. Technol. **11**, 475 (1996).
[6] G. Etemadi and J. F. Palmier, Sol. Stat. Comm. **86**, 739 (1993).
[7] G. Schwarz and E. Schöll, phys. status solidi (b) **194**, 351 (1996).